Title Page

Author names and affiliations: Nabodita Sinha[a], Avinash Y. Gahane[aΘ], Talat Zahra[aΘ], Ashwani K. Thakur[a*]

[a]Department of Biological Sciences and Bioengineering, Indian Institute of Technology Kanpur, UP-208016, India.

***Corresponding author:** Prof. A.K.Thakur (akthakur@iitk.ac.in)

[Θ] Equal contribution by authors

Title: Protein reservoirs of seeds are composites of amyloid and amyloid-like structures

Short title: Amyloidic nature of seed proteins

[a]The author(s) responsible for distribution of materials integral to the findings presented in this article in accordance with the policy described in the Instructions for Authors (https://academic.oup.com/plcell/pages/General-Instructions) is: Prof. A.K.Thakur (akthakur@iitk.ac.in).

[a]

Abstract

Seed storage proteins, well-known for their nutritional functions are sequestered in protein bodies. However, their biophysical properties at the molecular level remain elusive. Based on the structure and function of protein bodies found in other organisms, we hypothesize that the seed protein bodies might be present as amyloid structures. When visualized with a molecular rotor Thioflavin-T and a recently discovered Proteostat® probe with enhanced sensitivity, the seed sections showed amyloid-like signatures in the protein storage bodies of the aleurone cells of monocots and cotyledon cells of dicots. To make the study compliant for amyloid detection, gold-standard Congo red dye was used. Positive apple-green birefringence due to Congo red affinity in some of the areas of ThT and Proteostat® binding, suggests the presence of both amyloid-like and amyloid deposits in the protein storage bodies. Further, diminishing amyloid signature in germinating seeds implies the degradation of these amyloid structures and their utilization. This study will open new research avenues for a detailed molecular-level understanding of the formation and utilization of aggregated protein bodies as well as their evolutionary roles.

Introduction

The study of seed storage proteins in monocots can be traced back to 1745, when the isolation of wheat gluten was first described.(1) Analysis of dicot seed storage proteins initiated a century later with crystallization of Brazil nut globulins.(2) The discoveries were followed by detailed biochemical studies based on the extraction and solubility properties of the storage proteins.(1) The monocot seeds consist of the peripheral layers of aleurone and sub-aleurone cells, which have both storage and secretory functions.(3, 4) The endosperm cells on the other hand are solely for storage and are packed with starch and protein bodies.(5) In dicots, on the contrary, the cotyledon cells occupy the maximum volume of the seeds and are the sole reservoir cells.

The protein storage bodies of aleurone cells are mainly comprised of storage proteins such as 7S globulins. Proteomic analysis also suggests the presence of sequestered enzymes, heat shock proteins and defense peptides in these structures.(6) In addition, these protein bodies also contain inorganic mineral-rich globoids and lipid bodies.(7, 8) In dicot seeds, the

cotyledon cells are more or less uniform and contain starch granules embedded in a protein matrix.(9, 10) This protein matrix comprises of storage protein bodies and are mainly composed of aggregates of globulins including vicilin and legumin.(11, 12) Most of these storage proteins are targeted in association with the Golgi body, leading to the formation of aggregated electron-rich protein bodies.(1, 13, 14)

The protein bodies are not unique to plant seeds. Similar structures of electron-rich dense aggregates of proteins are found in diverse species, ranging from inclusion bodies of bacteria to Russell bodies of humans.(15) Interestingly, some of them also act as storage reservoirs. For example, metabolic enzymes assemble into aggregates in order to protect the proteins from stress in yeast,(16) while proteasome storage granules sequester and store the proteasomes for safe-keeping and recycling.(17) Sup35 in yeast still retains function in their aggregated state and acts as a translation release factor.(18)

Protein aggregates in general, can acquire multiple polymorphic structures. These include native reversible aggregates, partially unfolded globular protein aggregates, aggregate precursors (oligomers or protofibrils) and fibrillar aggregates including amyloids.(19, 20) The ultrastructural and biological properties of these aggregates depend on their type and pathway of formation. Although there has been reports suggesting disulfide bond formation, roles of molecular chaperones and specific protein-protein interaction resulting in the formation of the protein aggregates in the form of seed storage structures,(7) little is known about the biophysical aspects of these structures in terms of type of physical interactions, or aggregate types leading to amyloid formation tendencies. Considering the fact that the protein bodies of bacteria, yeast and even humans are often associated with amyloid or amyloid-like fibrils with high stability and similar functions of storage, we hypothesize that the plant seed protein bodies owing to their aggregation might possess amyloid or amyloid-like characteristics for performing functional roles.

To detect amyloids in plants, previous reports used heterologous systems of expression and experimental conditions to induce protein aggregation.(21) But these systems do not essentially reflect the inherent amyloid nature of the plant proteins *in-vivo*. In a recent study on vicilin, this protein is shown to be amyloidogenic by computational analysis, Thioflavin T (ThT) staining of seed section and *in-vitro* aggregation.(22) However, ThT alone is not enough to confirm amyloid presence and needs to be validated using orthogonal probes.

Moreover, the results obtained *in-vitro*, might not reflect the true behavior of these proteins in physiological context.

In order to detect amyloids on seed sections, we used two molecular rotors ThT and Proteostat®, which are popularly used for detection of amyloid or amyloid-like protein aggregates. Although ThT is popular for understanding aggregation kinetics, detection and quantification studies, it must be validated using novel probes with enhanced properties suited for biological samples. Proteostat® is a recently discovered molecular rotor and has higher specificity and sensitivity compared to ThT,(23) and this fluorogenic probe was further used to confirm ThT dataset. Moreover, to comply with the International Society of Amyloidosis (ISA) guidelines for amyloid detection in tissue sections and biological samples, Congo red staining was performed which is till date the 'gold standard' test for amyloids.(24) In this study, we have shown that the monocot seeds of wheat (*Triticum aestivum*), and barley (*Hordeum vulgare*) and dicot seeds of chickpea (*Cicer arietinum*) and mungbean (*Vigna radiata*) show intense amyloidic signatures in the protein storage bodies of the aleurone and cotyledon cells and the signals lose their intensity during seed germination, reflecting on the role of amyloids in nutrient mobilization.

Results

Acid fuchsin staining and SEM analysis of the protein storage bodies of monocot and dicot seeds: Amyloids are proteinaceous in nature and consist of cross-β sheet secondary structures, which provide stability to these aggregates. The other characteristic features of amyloids include increased resistance to detergents and proteases, ability to seed similar proteins and interaction with amyloid-specific dyes.(25) On the other hand, 'amyloid-like' fibrils are a diverse group that depicts some of the properties of 'amyloids' such as fibrillar morphology. However, these comprise aggregates that might lack one or more signatory characteristics of amyloids, but still can bind to amyloid-binding dyes such as ThT. These aggregates might also be comprised of metabolites, peptides or nucleobases.(26, 27) It is known that the aleurone and cotyledon cells possess protein storage bodies in the cytoplasm. However, before detecting amyloid presence, it is imperative to confirm the proteinaceous nature of these storage bodies and the integrity of the structure subsequent to sample processing and fixation for histology. Therefore, the monocot and dicot seed sections were stained with acid fuchsin to detect the proteinaceous regions. This also validates the earlier

findings of other researchers regarding the biochemical composition of these storage bodies. Moreover, to particularly decipher, the proteinaceous and carbohydrate-rich regions in seed sections, these were simultaneously stained with acid fuchsin and calcofluor white, respectively.

Acid fuchsin is a dye widely used in plant histochemical staining for protein-body rich regions (28, 29) Calcofluor white on the other hand, binds to β-glucan rich structures and emits blue fluorescence.(30) As shown in **Figure 1**, monocot seed sections of wheat and barley **(Figure 1 a and b)** and dicot seed sections of chickpea and mungbean **(Figure 1 c and d)** are stained with acid fuchsin. In monocot seeds, the seed coat, aleurone cell protein storage region and the endosperm matrix exhibit a magenta colour, characteristic of acid fuchsin stain. Whereas, in the dicot seeds, the cotyledon cells are stained light magenta except the starch granules which remain colorless, confirming the proteinaceous nature of the matrix on which starch granules are embedded. To further confirm the integrity and structural aspects, scanning electron microscopy (SEM) was performed on seed sections of wheat and mungbean. In the **Figure 1 e,** the dense granular cytoplasm of the intact aleurone cells is visible in wheat section. Mungbean cotyledon cells on the other hand, **(Figure 1 f)** show the cellular structure with starch granules visible on the protein storage matrix. Further, simultaneous staining with acid fuchsin and calcofluor white depicts the exact position of proteinaceous and carbohydrate-rich structures **(Figure S1).** In both aleurone cells **(Figure S1 a)** and cotyledon cells **(Figure S1 b),** the proteinaceous deposits fluoresce red due to acid fuchsin whereas the cell walls emit blue fluorescence.

Detection of amyloid-like deposits in the protein storage bodies of seeds by Thioflavin T staining: To demarcate the presence of amyloid or amyloid-like deposits in the seed storage structures, we chose Thioflavin T as the first probe for our study. This dye produces an intense fluorescence on binding with amyloid or amyloid-like aggregates,(31-33) and it remains till date as one of the most popular dyes for amyloid or amyloid-like deposit detection and for studying aggregation kinetics.(34-37)

For detecting amyloids or amyloid-like aggregates in seeds, the wheat **(Figure 2 a and b),** barley **(Figure 2 c and d),** chickpea **(Figure 2 f and g)** and mungbean **(Figure 2 h and i)** seed sections were stained with ThT and visualized using a Leica SP5 confocal microscope. In the monocot seeds, intense fluorescence intensity is observed in the aleurone layer as

compared to the endosperm. For further confirming this, the intensity of aleurone, sub-aleurone, and endosperm cells of the seed sections were analyzed by the Analysis function of ImageJ software. The average of five z-stack slice images is considered for this purpose. The graphs of wheat **(Figure 2 e)** and barley **(Figure 2 j)** show the intensity of aleurone to be significantly higher as compared to sub-aleurone layer and endosperm. In the dicot seed sections, the matrix of the cotyledon cells, containing protein storage bodies, produces an intense green fluorescence. Since both the aleurone and the cotyledon cells have aggregated bodies containing proteinaceous matter, high fluorescent intensity in these regions depict a significant binding of ThT to these protein reserves and confirms that the proteins are present as amyloids or amyloid-like fibrils.

Detection of amyloid deposits in the protein storage bodies of seeds by Proteostat® probe: To confirm further the presence of amyloidic protein storage aggregates in seeds, the ThT dataset was experimentally supported and validated by another molecular rotor Proteostat®, which has higher sensitivity as compared to ThT. It is a recently discovered probe, designed to detect intracellular and extracellular deposits of amyloids or amyloid-like deposits even if the amyloidogenic proteins are sparse in content.(38-40) Especially, the intracellular inclusions containing amyloid aggregates are efficiently detected.(41, 42)

Interestingly, when the monocot and dicot seed sections were stained with Proteostat®, the images show comparable pattern as similar to micrographs of ThT stained seed sections. In monocot seed sections of wheat **(Figure 3 a)** and barley **(Figure 3 b)**, the protein storage bodies of the aleurone layer is the area of maximum fluorescence intensity. In the chickpea **(Figure 3 c)** and mungbean **(Figure 3 d)** seed sections, the storage protein bodies of cotyledon cells produces a maximum fluorescence compared to cell walls and starch. This confirms and validates the presence of amyloids or amyloid-like aggregates in these particular regions.

Confirmation of amyloids by Congo red staining of monocot and dicot seed sections: The diagnostic relationship between amyloids and Congo red is historical and goes back to 1922 when this dye was used to stain amyloids and exhibited salmon-pink or red color in bright-field microscopy.(43) Subsequently, the optical anisotropy of amyloids on binding with Congo red and the resulting signature of apple-green birefringence enabled it as one of

the most reliable methods for detection of amyloids in clinical samples. It is still a method of choice recommended by the International Society of Amyloidosis (ISA) to detect amyloids and to distinguish these from amyloid-like fibrils.(24, 44) To confirm the presence of amyloid deposits in the storage bodies of aleurone and the cotyledon cells, monocot and dicot seed sections were stained with Congo red and the samples were visualized between two polarizers. As shown in **Figure 4**, a characteristic apple-green birefringence of amyloids was observed in the aleurone protein storage bodies of wheat **(Figure 4 a-d)** and barley **(Figure 4 e-h).** Fascinatingly, unlike ThT and Proteostat® staining, which showed intense signal in the entire aleurone cells, the Congo red induced birefringence was observed in some of the parts where ThT and Proteostat® shows signal. Similar case was observed for the cotyledon cells of chickpea **(Figure 4 i-l)** and mungbean **(Figure 4 m-p),** since birefringence was located at certain regions where ThT and Proteostat® binds in the storage protein bodies and did not cover the whole cell. Considering ThT, Proteostat® and Congo red staining, the results suggest that the protein storage bodies of the aleurone and the cotyledon cells are composites of amyloids and amyloid-like structures.

Amyloid detection and quantification in germinating seeds: Major changes in the histological and biochemical properties in seeds are observed in two stages – development and germination. To determine whether the amyloids can have functional implications, we stained the seed sections of barley and chickpea seeds with Congo red and ThT, after 48 hours of water imbibition. Congo red provides a qualitative approach and the seed sections in this case still showed apple-green birefringence, in the protein storage bodies of aleurone (**Figure 5 a and b)** and cotyledon cells **(Figure 5 c and d)**. To quantitate the changes due to germination, the seed sections were stained with ThT and images were recorded using wide-field fluorescence microscope Leica DM 2500. As shown in **Figure 5,** barley non-germinated seed shows a higher fluorescence intensity in the aleurone layer **(Figure 5 e)** as compared to germinated seed **(Figure 5 f)**. On similar lines, the cotyledon cells of non-germinated seed of chickpea **(Figure 5 g)** shows more intense signal as compared to germinated seed **(Figure 5 h).** The change in intensity in the aleurone and cotyledon cells was calculated for germinated vs. non-germinated seeds by keeping similar imaging parameters. The normalized intensity values were plotted **(Figure 5 i).** It is evident from the plot that the amyloid signature intensity in the germinated seeds is significantly lower in both monocots and dicots, hinting towards the functional role of amyloid degradation for seed germination.

Discussion

Amyloids are well-known for their pathogenic and functional roles in diverse organisms.(45) In humans, more than 35 amyloid proteins are known to cause diseases and result in high mortality rate. Amyloids also offer protective roles in several species due to their high stability, defense properties and adhesive nature.(46) This paradoxical nature of the amyloids has gained significant attention in the last decades for biomaterial and therapeutic development and also for deciphering the mechanistic pathways.(47)

Despite of some perspectives, reviews and reports regarding plausible presence of amyloids in plants, till date there has not been many studies for detection of amyloids in seeds.(22) Although multiple plant proteins have been shown to form amyloids in heterologous expression systems,(21) but they may not necessarily reflect the behaviour of the endogenous proteins. Moreover, no study has employed a combinatorial approach with latest probes such as Proteostat® and the standard Congo red assay for amyloid detection in seed sections. This is indeed surprising, since Congo red remains as the 'gold standard' assay for detection of amyloids in tissues.(24) One possible reason for this might be the fact that Congo red also binds to cellulose and lignin and exhibits apple-green birefringence similar to amyloids. However, since in the seed reservoir cells, the exact location of the cell walls is known, any amyloid signature in the cells can be safely ascribed to proteinaceous deposits, owing to the fact that starch, the other major component of seed reservoir cells, does not bind to Congo red. To confirm this further, we performed dual staining of seed sections of barley and mungbean with acid fuchsin and calcofluor white. The former fluoresces bright red on binding with proteins whereas the latter dye emits blue fluorescence on binding with β-glucan rich carbohydrate structures. The micrographs further confirm that the areas where we have seen binding with amyloid-specific dyes, vis-à-vis the aleurone and cotyledon cell protein storage bodies, belong to proteinaceous deposits and not carbohydrates. Moreover, orthogonal staining systems provide advantages since molecular rotors such as ThT and Proteostat® binding mode to amyloids differs from Congo red binding. Amyloids or amyloid-like aggregates due to their ordered structure can sterically lock the bound ThT molecules in their grooves, resulting in certain rotational conformations of ThT, which increases the fluorescence as compared to free ThT molecules.(48, 49) On the other hand, Congo red is a planar dye that is oriented at an oblique angle to the aggregates. This allows interaction with

nearby Congo red molecules and facilitates a cooperative mechanism of binding.(50) Moreover, the amyloidic nature of the aggregates need further classification as to whether they are amyloid or amyloid-like. Whereas amyloids are proteinaceous cross-β sheet rich aggregates, resistant to detergents and enzymes and have the ability to induce aggregation of similar proteins, amyloid-like aggregates on the other hand may or may not contain protein, and might lack one or more of the key characteristics of amyloids. While ThT is seen to bind to both amyloid and amyloid-like aggregates, Congo red is often the molecule of choice for confirmation of amyloid presence in tissues.(27) Thus, experimental validation using multiple amyloid-specific dyes is imperative to confirm the presence of amyloids in any biological sample.

The protein bodies found in the seed reservoir cells, are similar to amyloidic protein bodies of other organisms, and also perform similar functions of storage and sequestration.(16) Therefore, we hypothesized that the protein reservoir cells of monocot and dicot seeds might contain amyloid deposits. To confirm this hypothesis, we chose wheat and barley as monocots, and chickpea and mungbean seeds as dicot representatives. The seeds were first analysed for their integrity, and presence of proteins, following tissue processing and fixation. For this purpose, the seed sections were analysed by SEM and stained with acid fuchsin, a protein-specific dye. The stained sections of monocots and dicots showed acid fuchsin staining in aleurone and cotyledon cells. SEM analysis also depicts the integrity of the tissue architecture and structure of the intact cells. To confirm the presence of amyloids or amyloid-like aggregates in proteinaceous deposits showing positive affinity with acid fuchsin, the samples were stained with two fluorescent dyes – ThT and Proteostat®, that are known to bind with amyloids or amyloid-like fibrils. Intriguingly, we found strong signal intensity in the peripheral tissues and especially in the aleurone cells of the monocots, indicative of amyloids or amyloid–like deposits. In dicot cotyledon cells, both the fluoregenic dyes produced intense signal in the protein storage bodies of each cotyledon cell. To confirm the results further, we used Congo red stain as amyloid-specific dye for tissues. Fascinatingly, whereas ThT and Proteostat® bound to the entire aleurone cell's and cotyledon cell's cytoplasm, the birefringent signals of amyloid due to Congo red staining appeared in some specific areas among these proteinaceous regions. Thus it might be concluded that the storage protein bodies of aleurone layer and cotyledon cells are comprised of both amyloid and amyloid-like deposits. The endosperm cells of the monocots however showed a much lower amyloidic signature with the dyes.

The theory of the amyloid presence in specifically seed reservoir cells has manifold implications in seed properties and functions. Since amyloid formation follows well-defined pathways of nucleation and elongation in most of the systems studied,(51) these models can also be used to explain the biogenesis of the protein bodies and their aggregation by probable self-seeding and sequestration of other protein components. Moreover, since the amyloids are known for their exceptionally stable nature(52) including high mechanical strength and resistance to common protease enzymes and detergents, the presence of these structures in the seeds might facilitate protection from environmental stress. We have shown here one such possible functional implication by comparing the amyloids in germinated and non-germinated seeds qualitatively and quantitatively. The quantitative analysis shows a decrease in intensity of ThT fluorescence of germinated seeds, suggesting degradation of amyloids during germination. A similar hypothesis was recently proposed in a recent spotlight article.(53)

The current study sheds light on the potential amyloidic nature of the composites found in the storage protein cells of seed using a combinatorial approach of novel and established amyloid probes. This would open up a new avenue of research by making it imperative to study in details the ultrastructure, biophysical and functional properties of plant amyloids. Further, the biogenesis of amyloid containing protein bodies can be mimicked *in-vitro* and *in-vivo* to investigate common model of amyloid formation. The seeding and sequestration effects of the plant amyloids, if established might explain stability of plant seeds to environmental stresses and may even illuminate the enigmatic issue of the role of functional amyloids in evolution across species.

Methods

Materials used: Seeds of wheat (*Triticum aestivum*), barley (*Hordeum vulgare*), chickpea (*Cicer arietinum*) and mungbean (*Vigna radiata*) were used for the experiments. Congo red, Thioflavin-T, and acid fuchsin were obtained from Sigma Aldrich. Proteostat® aggregation assay kit was obtained from Enzo Life Sciences. Calcofluor white, xylene, ethanol and neutral buffered formalin (4%) were procured from Thermo Scientific. Leica paraffin wax is used for embedding and Superfrost microscopic slides for histochemical staining were from HiMedia. Leica Microtome was used to obtain all the sections. The sections of all the seeds had a thickness of 8 µm. Visualization was enabled by Leica DM 2500 widefield fluorescent microscope equipped with cross-polarizers and Leica SP5 confocal microscope.

Sectioning of the seeds: The processing was done as per the standard protocols (54, 55) and was optimized to facilitate staining and visualization with different dyes. Briefly, the seeds were washed, surface-sterilized, cut in half using scalpels and incubated in 4% neutral buffered formalin at room temperature for 2 hours. The samples were then transferred to 4˚C for overnight fixation. After washing the fixed seeds 2-3 times with phosphate buffered saline solution, the samples were dehydrated with successive gradients of ethanol (30%, 50%, 70%, 90%), with each ethanol gradient treatment for 30 minutes. Gradient dehydration was followed by treatment of the samples with 100% ethanol twice, for 1 hour each. The samples were then permeated with xylene followed by a mixture of xylene and paraffin in the ratio of 1:1 for 1 hour. The xylene was discarded and paraffin embedding was continued by incubating overnight at 60˚C. The sections were then transferred to paraffin blocks and stored at 4˚C for further use. From the blocks, 8 µm sections were cut and were carefully transferred to glass slides. The slides were heat-fixed on hot plates for 30 minutes at 60˚C and stored at 4˚C for further use. For germination study, the seeds were imbibed in cotton soaked with water under a light/dark cycle of 12/12 hours. After imbibition, the same procedure for fixation and processing was done.

Histochemical staining of tissue sections: The processed slides were heated for 2-3 minutes at 70˚C and immediately transferred to xylene for 2 minutes in coplin jars. The slides were treated with successive gradients of ethanol (100%, 95%, and 70%) for 5 minutes each. For 95% and 70% alcohol concentrations, the treatments were repeated once. The slides are then washed with distilled water for 10 minutes.

For **SEM** analysis, after water wash, the slides are air-dried and dehydrated in a vacuum desiccator overnight. The samples are then sputter-coated with gold and visualized by Carl Zeiss Evo 18 SEM (10 kV).

For staining, the slides after water wash are dipped in coplin jars containing the staining solution. Acid fuchsin (0.35%) and Calcofluor white (10% v/v) stain was applied on the slides for 1 minute. Saturated solution of Congo red was used for amyloid detection by incubating the slides in the staining solution for 20 minutes. Proteostat® dye was reconstituted (75 µL) in 10 ml of 1X assay buffer according to the manufacturer's protocol. For ThT (20µM) and Proteostat® staining, 10 µL of the dye was added on the tissue sections.

Acid fuchsin stained sections were visualized under bright-field and wide-field fluorescence microscopy using the red filter. Calcofluor white was observed using the blue emission filter.

Birefringence and Congo red binding were observed using bright-field microscopy and by rotating the polarisers. Proteostat® was observed using the red emission filter of a Leica DM 2500 wide-field fluorescence microscope at 40X air objective. ThT signal of seed sections was visualized by Leica TCS SP5 confocal system using He-Ne 488 laser (at 20% laser power) at 10X and 40X (under oil emersion). For each magnification, ˜40 z-stacks were collected. Quantification of the ThT signal was performed by measuring the ratio of intensity to area for selected areas of each type of tissue using ImageJ analysis. For this, 5 stacks were considered for each seed section. For germination study, the seed sections were stained with Congo red and ThT. The birefringence due to Congo red staining was observed using polariser microscope. ThT signal in this case, was visualized using Leica DM 2500 widefield fluorescence microscope using green emission filter. The intensity for three areas of each section was measured and normalized to area to calculate changes in intensity using ImageJ. The graphs were plotted using Origin Pro 9.1. All experiments were repeated thrice for statistically significant results.

Supplemental data files:

1. Figure S1 Acid fuchsin and calcofluor staining to demarcate the proteinaeous and carbohydrate-rich regions

Acknowledgements: We are thankful to Prof. Pradip Sinha and Prof. Amitabha Bandyopadhyay for letting us use their confocal imaging facility and ultramicrotome facility. We also thank Mr. Upendra Singh Yadav and Mr. Saurabh Singh Parihar for helping with the facilities. N.S and T.Z. acknowledge University Grants Commission for Senior Research Fellowship.

Author Contributions: The study was conceptualized by A.K.T. The experiments were designed by N.S, A.Y.G and A.K.T. The experiments were performed by N.S., T.Z and A.Y.G. Paper was written by N.S. and A.K.T. Data was analysed by all authors.

References:

1. Shewry PR, Halford NG. Cereal seed storage proteins: structures, properties and role in grain utilization. Journal of experimental botany. 2002;53(370):947-58.
2. Shewry PR, Napier JA, Tatham AS. Seed storage proteins: structures and biosynthesis. The Plant cell. 1995;7(7):945-56.
3. Tosi P, Gritsch CS, He J, Shewry PR. Distribution of gluten proteins in bread wheat (Triticum aestivum) grain. Annals of botany. 2011;108(1):23-35.
4. Xiong F, Yu XR, Zhou L, Wang Z, Wang F, Xiong AS. Structural development of aleurone and its function in common wheat. Molecular biology reports. 2013;40(12):6785-92.
5. Buttrose M. Ultrastructure of the Developing Aleurone Cells of Wheat Grain. Australian Journal of Biological Sciences. 1963;16(4):768-74.
6. Nadaud I, Tasleem-Tahir A, Chateigner-Boutin A-L, Chambon C, Viala D, Branlard G. Proteome evolution of wheat (Triticum aestivum L.) aleurone layer at fifteen stages of grain development. Journal of Proteomics. 2015;123:29-41.
7. Reyes FC, Chung T, Holding D, Jung R, Vierstra R, Otegui MS. Delivery of Prolamins to the Protein Storage Vacuole in Maize Aleurone Cells. The Plant Cell. 2011;23(2):769-84.
8. BETHKE PC, SWANSON SJ, HILLMER S, JONES RL. From Storage Compartment to Lytic Organelle: The Metamorphosis of the Aleurone Protein Storage Vacuole. Annals of Botany. 1998;82(4):399-412.
9. Hughes JS, Swanson B. MICROSTRUCTURE OF LENTIL SEEDS (Lens Culinaris). Food Structure. 1986;5:8.
10. Brillouet J-M, Carré B. Composition of cell walls from cotyledons of Pisum sativum, Vicia faba and Glycine max. Phytochemistry. 1983;22(4):841-7.
11. Derbyshire E, Wright DJ, Boulter D. Legumin and vicilin, storage proteins of legume seeds. Phytochemistry. 1976;15(1):3-24.
12. Craig S, Millerd A. Pea seed storage proteins — Immunocytochemical localization with protein a-gold by electron microscopy. Protoplasma. 1981;105(3):333-9.
13. Abirached-Darmency M, Dessaint F, Benlicha E, Schneider C. Biogenesis of protein bodies during vicilin accumulation in Medicago truncatula immature seeds. BMC Research Notes. 2012;5(1):409.
14. Herman E, Schmidt M. Endoplasmic Reticulum to Vacuole Trafficking of Endoplasmic Reticulum Bodies Provides an Alternate Pathway for Protein Transfer to the Vacuole. Plant Physiology. 2004;136(3):3440-6.
15. Schmidt SR. Protein Bodies in Nature and Biotechnology. Molecular Biotechnology. 2013;54(2):257-68.
16. Narayanaswamy R, Levy M, Tsechansky M, Stovall GM, O'Connell JD, Mirrielees J, et al. Widespread reorganization of metabolic enzymes into reversible assemblies upon nutrient starvation. Proceedings of the National Academy of Sciences. 2009;106(25):10147-52.
17. Peters LZ, Karmon O, David-Kadoch G, Hazan R, Yu T, Glickman MH, et al. The Protein Quality Control Machinery Regulates Its Misassembled Proteasome Subunits. PLOS Genetics. 2015;11(4):e1005178.
18. Pezza JA, Villali J, Sindi SS, Serio TR. Amyloid-associated activity contributes to the severity and toxicity of a prion phenotype. Nature Communications. 2014;5(1):4384.
19. Chiti F, Dobson CM. Protein Misfolding, Functional Amyloid, and Human Disease. Annual Review of Biochemistry. 2006;75(1):333-66.
20. Dobson CM. The Amyloid Phenomenon and Its Links with Human Disease. Cold Spring Harbor perspectives in biology. 2017;9(6):a023648.
21. Antonets KS, Nizhnikov AA. Amyloids and prions in plants: Facts and perspectives. Prion. 2017;11(5):300-12.

22. Antonets KS, Belousov MV, Sulatskaya AI, Belousova ME, Kosolapova AO, Sulatsky MI, et al. Accumulation of storage proteins in plant seeds is mediated by amyloid formation. PLoS Biol. 2020;18(7):e3000564.
23. Shen D, Coleman J, Chan E, Nicholson TP, Dai L, Sheppard PW, et al. Novel cell- and tissue-based assays for detecting misfolded and aggregated protein accumulation within aggresomes and inclusion bodies. Cell Biochem Biophys. 2011;60(3):173-85.
24. Benson MD, Buxbaum JN, Eisenberg DS, Merlini G, Saraiva MJM, Sekijima Y, et al. Amyloid nomenclature 2020: update and recommendations by the International Society of Amyloidosis (ISA) nomenclature committee. Amyloid : the international journal of experimental and clinical investigation : the official journal of the International Society of Amyloidosis. 2020;27(4):217-22.
25. Biancalana M, Makabe K, Koide S. Minimalist design of water-soluble cross-β architecture. Proceedings of the National Academy of Sciences. 2010;107(8):3469-74.
26. Shaham-Niv S, Rehak P, Zaguri D, Levin A, Adler-Abramovich L, Vuković L, et al. Differential inhibition of metabolite amyloid formation by generic fibrillation-modifying polyphenols. Communications Chemistry. 2018;1(1):25.
27. Matiiv AB, Trubitsina NP, Matveenko AG, Barbitoff YA, Zhouravleva GA, Bondarev SA. Amyloid and Amyloid-Like Aggregates: Diversity and the Term Crisis. Biochemistry (Moscow). 2020;85(9):1011-34.
28. Nielsen LF, Moe D, Kirkeby S, Garbarsch C. Sirius red and acid fuchsin staining mechanisms. Biotechnic & histochemistry : official publication of the Biological Stain Commission. 1998;73(2):71-7.
29. Irving DW. Seed Structure and Histochemistry of Prosopis velutina (Leguminosae). Botanical Gazette. 1984;145(3):340-5.
30. Herrera-Ubaldo H, de Folter S. Exploring Cell Wall Composition and Modifications During the Development of the Gynoecium Medial Domain in Arabidopsis. Frontiers in Plant Science. 2018;9(454).
31. Biancalana M, Koide S. Molecular mechanism of Thioflavin-T binding to amyloid fibrils. Biochimica et biophysica acta. 2010;1804(7):1405-12.
32. LeVine H, 3rd. Thioflavine T interaction with synthetic Alzheimer's disease beta-amyloid peptides: detection of amyloid aggregation in solution. Protein science : a publication of the Protein Society. 1993;2(3):404-10.
33. Xue C, Lin TY, Chang D, Guo Z. Thioflavin T as an amyloid dye: fibril quantification, optimal concentration and effect on aggregation. R Soc Open Sci. 2017;4(1):160696.
34. Chiti F, Dobson CM. Protein Misfolding, Amyloid Formation, and Human Disease: A Summary of Progress Over the Last Decade. Annual Review of Biochemistry. 2017;86(1):27-68.
35. Biancalana M, Koide S. Molecular mechanism of Thioflavin-T binding to amyloid fibrils. Biochimica et Biophysica Acta (BBA) - Proteins and Proteomics. 2010;1804(7):1405-12.
36. Boke E, Ruer M, Wühr M, Coughlin M, Lemaitre R, Gygi SP, et al. Amyloid-like Self-Assembly of a Cellular Compartment. Cell. 2016;166(3):637-50.
37. Tayeb-Fligelman E, Tabachnikov O, Moshe A, Goldshmidt-Tran O, Sawaya MR, Coquelle N, et al. The cytotoxic Staphylococcus aureus PSMα3 reveals a cross-α amyloid-like fibril. Science (New York, NY). 2017;355(6327):831-3.
38. Navarro S, Ventura S. Fluorescent dye ProteoStat to detect and discriminate intracellular amyloid-like aggregates in Escherichia coli. Biotechnology Journal. 2014;9(10):1259-66.
39. Oshinbolu S, Shah R, Finka G, Molloy M, Uden M, Bracewell DG. Evaluation of fluorescent dyes to measure protein aggregation within mammalian cell culture supernatants. J Chem Technol Biotechnol. 2018;93(3):909-17.
40. Laor D, Sade D, Shaham-Niv S, Zaguri D, Gartner M, Basavalingappa V, et al. Fibril formation and therapeutic targeting of amyloid-like structures in a yeast model of adenine accumulation. Nature Communications. 2019;10(1):62.

41. Navarro S, Ventura S. Fluorescent dye ProteoStat to detect and discriminate intracellular amyloid-like aggregates in Escherichia coli. Biotechnology Journal. 2014;9.
42. Zhao Z, Cao L, Reece EA. Formation of neurodegenerative aggresome and death-inducing signaling complex in maternal diabetes-induced neural tube defects. Proceedings of the National Academy of Sciences. 2017;114(17):4489-94.
43. Yakupova Elmira I, Bobyleva Liya G, Vikhlyantsev Ivan M, Bobylev Alexander G. Congo Red and amyloids: history and relationship. Bioscience Reports. 2019;39(1).
44. Murphy CL, Eulitz M, Hrncic R, Sletten K, Westermark P, Williams T, et al. Chemical typing of amyloid protein contained in formalin-fixed paraffin-embedded biopsy specimens. American journal of clinical pathology. 2001;116(1):135-42.
45. Bleem A, Daggett V. Structural and functional diversity among amyloid proteins: Agents of disease, building blocks of biology, and implications for molecular engineering. Biotechnology and Bioengineering. 2017;114(1):7-20.
46. Otzen D, Riek R. Functional Amyloids. Cold Spring Harbor perspectives in biology. 2019;11(12).
47. Kumar V, Sinha N, Thakur AK. Necessity of regulatory guidelines for the development of amyloid based biomaterials. Biomaterials science. 2021;9(12):4410-22.
48. Voropai ES, Samtsov MP, Kaplevskii KN, Maskevich AA, Stepuro VI, Povarova OI, et al. Spectral Properties of Thioflavin T and Its Complexes with Amyloid Fibrils. Journal of Applied Spectroscopy. 2003;70(6):868-74.
49. Sulatskaya AI, Kuznetsova IM, Belousov MV, Bondarev SA, Zhouravleva GA, Turoverov KK. Stoichiometry and Affinity of Thioflavin T Binding to Sup35p Amyloid Fibrils. PLOS ONE. 2016;11(5):e0156314.
50. Espargaró A, Llabrés S, Saupe SJ, Curutchet C, Luque FJ, Sabaté R. On the Binding of Congo Red to Amyloid Fibrils. Angewandte Chemie International Edition. 2020;59(21):8104-7.
51. Bhattacharyya AM, Thakur AK, Wetzel R. Polyglutamine aggregation nucleation: Thermodynamics of a highly unfavorable protein folding reaction. Proceedings of the National Academy of Sciences. 2005;102(43):15400-5.
52. Makin OS, Atkins E, Sikorski P, Johansson J, Serpell LC. Molecular basis for amyloid fibril formation and stability. Proceedings of the National Academy of Sciences of the United States of America. 2005;102(2):315-20.
53. Santos J, Ventura S. Functional Amyloids Germinate in Plants. Trends in Plant Science. 2021;26(1):7-10.
54. Jääskeläinen A-S, Holopainen-Mantila U, Tamminen T, Vuorinen T. Endosperm and aleurone cell structure in barley and wheat as studied by optical and Raman microscopy. Journal of Cereal Science. 2013;57(3):543-50.
55. Wood JA, Knights EJ, Choct M. Morphology of Chickpea Seeds (Cicer arietinum L.): Comparison of desi and kabuli Types. International Journal of Plant Sciences. 2011;172(5):632-43.

Figure legends:

Figure 1 Acid fuchsin staining and SEM analysis of monocot and dicot seed sections. The protein-specific dye, acid fuchsin exhibits characteristic magenta color in the seed coat (black solid arrow), aleurone (black dashed boxes) and sub-aleurone layer (black dashed arrow) of wheat (*Triticum aestivum*) (a) and barley (*Hordeum vulgare*) (b). In the dicot seeds, the stain is visible in the protein storage bodies of cotyledon cells (black dashed boxes) of chickpea (*Cicer arietinum*) (c) and mungbean (*Vigna radiata*) (d). Acid fuchsin stains the aleurone and cotyledon cells prominently, exhibiting the proteinaceous deposits in these cells. SEM (Scanning Electron Microscopy) analysis of wheat (e) and mungbean (f) reveal that the structure of the aleurone and cotyledon cells are maintained after histological processing. (Gamma value for each bright-field image ranges from 0.6-0.9, the changes in brightness/contrast has been applied to whole image)

Figure 2 Thioflavin T stained sections of monocot and dicot seed. Both wheat (*Triticum aestivum*) (a, b and e) and barley (*Hordeum vulgare*) (c, d and j) exhibit an intense fluorescence in the aleurone layer as compared to the endosperm cells, suggesting an enrichment of amyloid-like protein aggregates in these regions. The dicot seeds of chickpea (*Cicer arietinum*) (f and g) and mungbean (*Vigna radiata*) (h and i) exhibit an intense signal in the protein storage bodies of cotyledons. The white dashed boxes represent intense fluorescing areas of 10X magnified images and white solid lined boxes represent similar areas in 40X magnified images. The insets represent magnified portions of the solid lined boxes. (*$p<0.05$, **$p<0.01$) (Gamma and intensity value for each confocal image is kept same for quantification purpose)

Figure 3 Proteostat® stained sections of monocots and dicots to confirm the presence of amyloidic aggregates. The monocot seeds wheat (*Triticum aestivum*) (a) and barley (*Hordeum vulgare*) (b) and dicot seeds of chickpea (*Cicer arietinum*) (c) and mungbean (*Vigna radiata*) (d), demonstrate the presence of possible amyloids or amyloid-like aggregates in the protein storage bodies of aleurone and cotyledon cells as evident from the red fluorescence in these areas. (Gamma values for each image ranges from 0.8-2.5 to bring uniformity, changes in brightness/contrast has been applied to whole image)

Figure 4 Congo red stained sections of monocot and dicot seeds to confirm amyloids. Left two panels represent the apple-green to red birefringence when the sample is placed between two polarisers at 10X magnification. The right two panels show the same at 40X magnification. Both wheat (*Triticum aestivum*) (a-d) and barley (*Hordeum vulgare*) (e-h) aleurone cells show a visible change in the apple-green birefringence, characteristic of amyloids as indicated by the white dashed boxes inside the insets**.** Similar changes in birefringence are observed in some regions of the protein storage bodies of cotyledon cells of chickpea (i-l) (*Cicer arietinum*) and mungbean (*Vigna radiata*) (m-p). (Gamma values for 10X panels vary from 0.6-1.21, while for 40X panel, Gamma ranges from 0.5-0.9 for facilitating clear birefringence visualization, no changes in imaging parameters were done while rotating polarizer; the insets have been enhanced regarding brightness/contrast for clear presentation)

Figure 5 Congo red and Thioflavin T (ThT) staining of germinated monocot and dicot seeds and quantification of amyloid signature. In both barley (*Hordeum vulgare*) (a and b) and chickpea (*Cicer arietinum*) (c and d), Congo red staining of both non-germinated and germinated seed tissue sections exhibit amyloid signatures. ThT staining of non-germinated seeds of barley (e) and chickpea (g) show an apparent higher fluorescence intensity compared to germinated sections of barley (f) and chickpea (h) respectively. The fluorescence intensity is plotted (i) and shows significant decrease in amyloid signature in germinated seeds as compared to non-germinated ones. (*$p<0.05$) (Gamma for Congo red stained sections are in the range of 0.5-0.6, For quantification purpose by ThT, the Gamma value of barley germinated and non-germinated seed both were 1.82, for chickpea Gamma was 2.03, to avoid discrepancies in quantification)

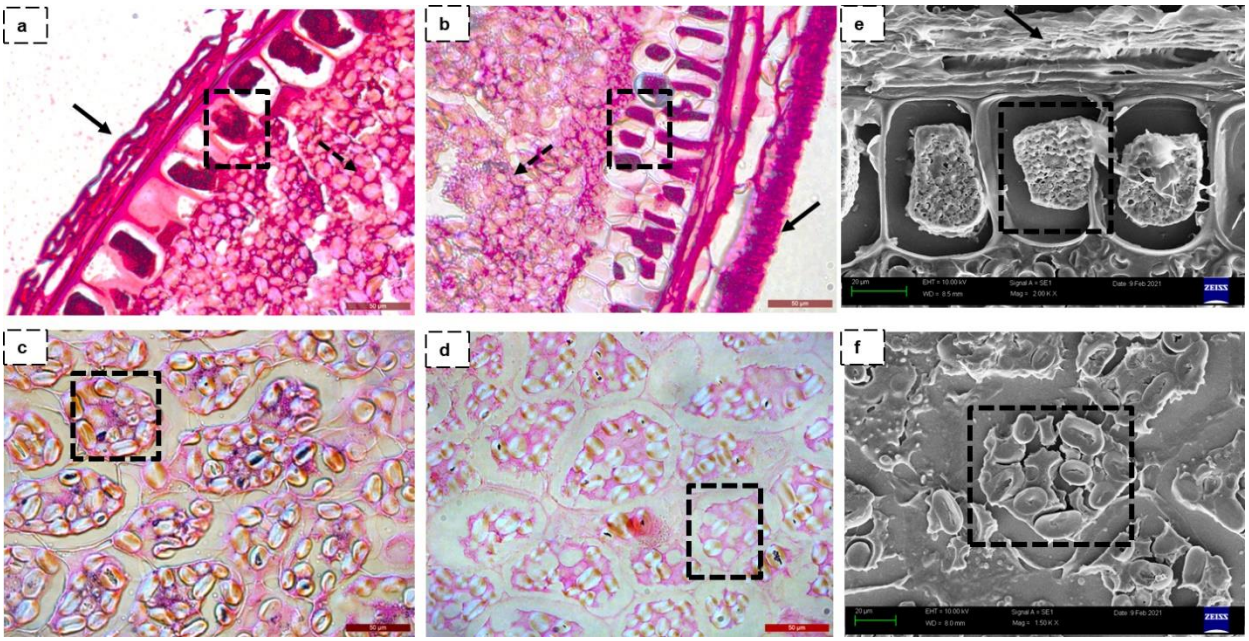

Figure 1 Acid fuchsin staining and SEM analysis of monocot and dicot seed sections. The protein-specific dye, acid fuchsin exhibits characteristic magenta color in the seed coat (black solid arrow), aleurone (black dashed boxes) and sub-aleurone layer (black dashed arrow) of wheat (*Triticum aestivum*) (a) and barley (*Hordeum vulgare*) (b). In the dicot seeds, the stain is visible in the protein storage bodies of cotyledon cells (black dashed boxes) of chickpea (*Cicer arietinum*) (c) and mungbean (*Vigna radiata*) (d). Acid fuchsin stains the aleurone and cotyledon cells prominently, exhibiting the proteinaceous deposits in these cells. SEM (Scanning Electron Microscopy) analysis of wheat (e) and mungbean (f) reveal that the structure of the aleurone and cotyledon cells are maintained after histological processing. (Gamma value for each bright-field image ranges from 0.6-0.9, the changes in brightness/contrast has been applied to whole image)

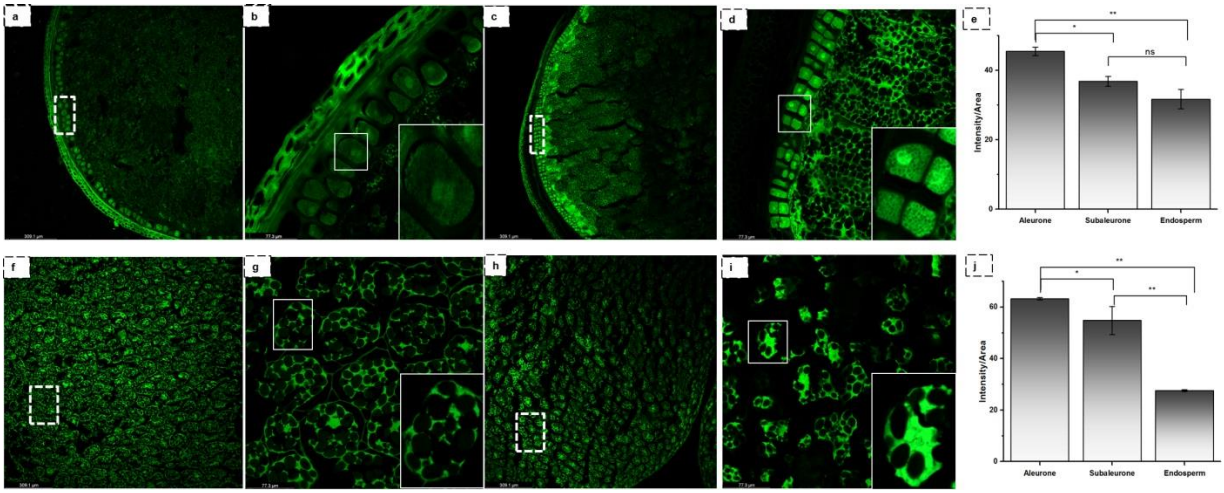

Figure 2 Thioflavin T stained sections of monocot and dicot seed. Both wheat (*Triticum aestivum*) (a, b and e) and barley (*Hordeum vulgare*) (c, d and j) exhibit an intense fluorescence in the aleurone layer as compared to the endosperm cells, suggesting an enrichment of amyloid-like protein aggregates in these regions. The dicot seeds of chickpea (*Cicer arietinum*) (f and g) and mungbean (*Vigna radiata*) (h and i) exhibit an intense signal in the protein storage bodies of cotyledons. The white dashed boxes represent intense fluorescing areas of 10X magnified images and white solid lined boxes represent similar areas in 40X magnified images. The insets represent magnified portions of the solid lined boxes. (*p<0.05, **p<0.01) (Gamma and intensity value for each confocal image is kept same for quantification purpose)

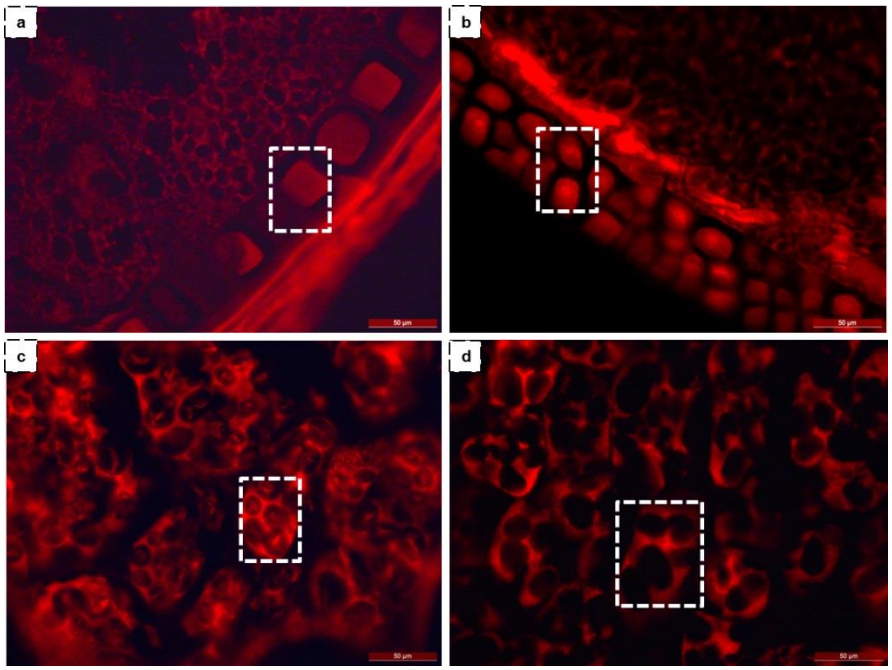

Figure 3 Proteostat® stained sections of monocots and dicots to confirm the presence of amyloidic aggregates. The monocot seeds wheat (*Triticum aestivum*) (a) and barley (*Hordeum vulgare*) (b) and dicot seeds of chickpea (*Cicer arietinum*) (c) and mungbean (*Vigna radiata*) (d), demonstrate the presence of possible amyloids or amyloid-like aggregates in the protein storage bodies of aleurone and cotyledon cells as evident from the red fluorescence in these areas. (Gamma values for each image ranges from 0.8-2.5 to bring uniformity, changes in brightness/contrast has been applied to whole image)

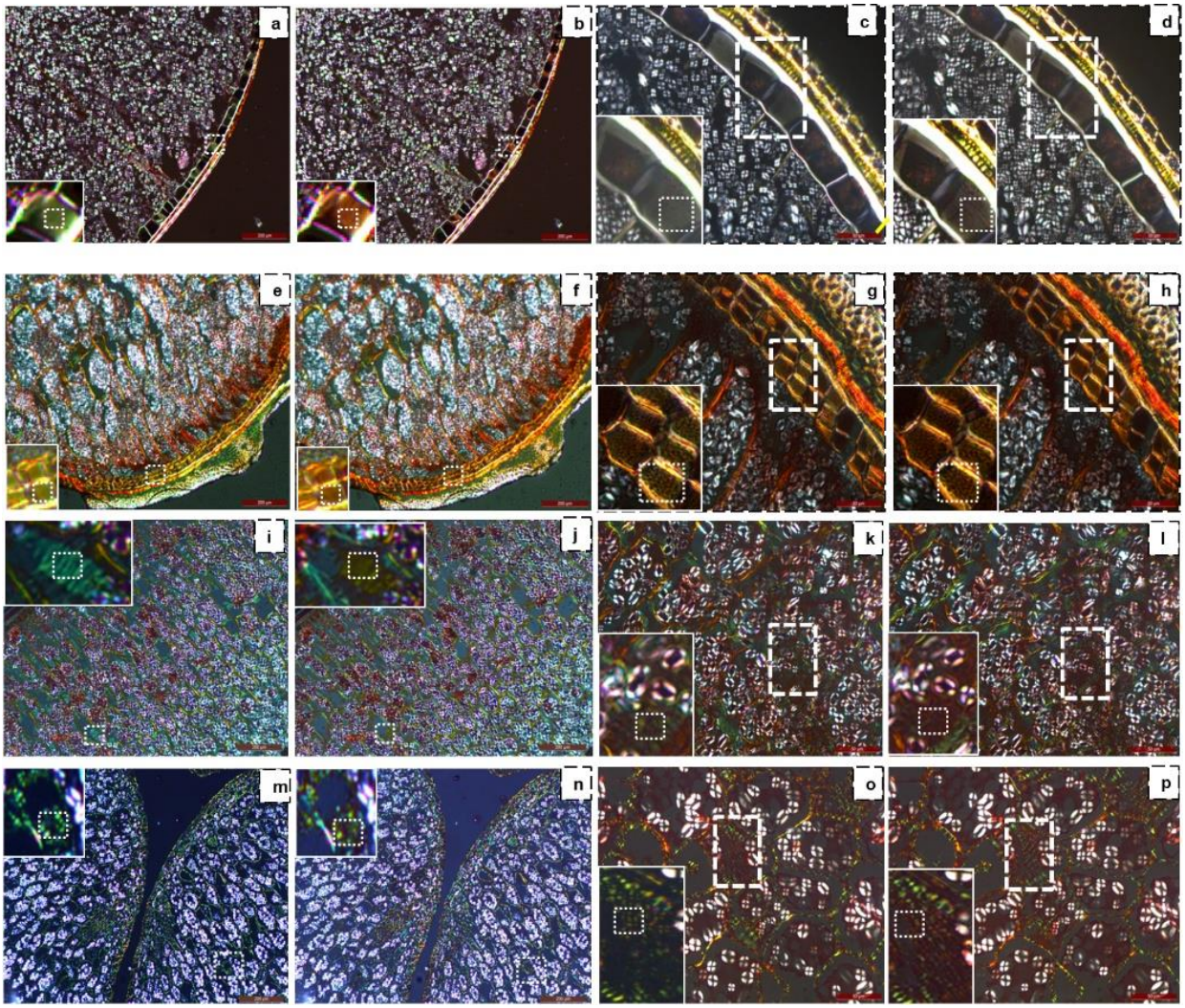

Figure 4 Congo red stained sections of monocot and dicot seeds to confirm amyloids. Left two panels represent the apple-green to red birefringence when the sample is placed between two polarisers at 10X magnification. The right two panels show the same at 40X magnification. Both wheat (*Triticum aestivum*) (a-d) and barley (*Hordeum vulgare*) (e-h) aleurone cells show a visible change in the apple-green birefringence, characteristic of amyloids as indicated by the white dashed boxes inside the insets**.** Similar changes in birefringence are observed in some regions of the protein storage bodies of cotyledon cells of chickpea (i-l) (*Cicer arietinum*) and mungbean (*Vigna radiata*) (m-p). (Gamma values for 10X panels vary from 0.6-1.21, while for 40X panel, Gamma ranges from 0.5-0.9 for facilitating clear birefringence visualization, no changes in imaging parameters were done while rotating polarizer; the insets have been enhanced regarding brightness/contrast for clear presentation)

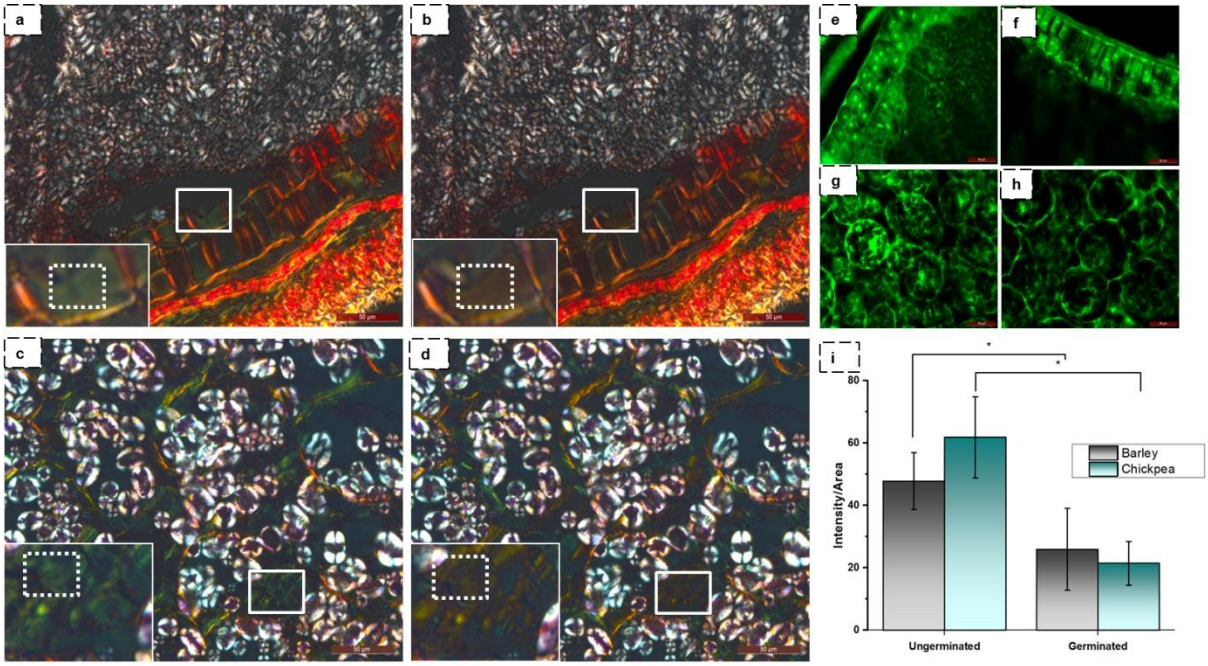

Figure 5 Congo red and Thioflavin T (ThT) staining of germinated monocot and dicot seeds and quantification of amyloid signature. In both barley (*Hordeum vulgare*) (a and b) and chickpea (*Cicer arietinum*) (c and d), Congo red staining of both non-germinated and germinated seed tissue sections exhibit amyloid signatures. ThT staining of non-germinated seeds of barley (e) and chickpea (g) show an apparent higher fluorescence intensity compared to germinated sections of barley (f) and chickpea (h) respectively. The fluorescence intensity is plotted (i) and shows significant decrease in amyloid signature in germinated seeds as compared to non-germinated ones. (*$p<0.05$) (Gamma for Congo red stained sections are in the range of 0.5-0.6, For quantification purpose by ThT, the Gamma value of barley germinated and non-germinated seed both were 1.82, for chickpea Gamma was 2.03, to avoid discrepancies in quantification)